Pergamon

0006-2952(95)00206-5

Biochemical Pharmacology, Vol. 50, No. 6, pp. 823–831, 1995.

0006-2952/95 $9.50 + 0.00

VIRTUAL KINETICS: USING STATISTICAL EXPERIMENTAL DESIGN FOR RAPID ANALYSIS OF ENZYME INHIBITOR MECHANISMS

DUANE D. BRONSON,*† DONNA M. DANIELS,* JEFFREY T. DIXON,* CATHERINE C. REDICK* and PERRY D. HAALAND‡

*Protein Chemistry, Sphinx Pharmaceuticals, Division of Eli Lilly, Durham, NC 27717; and ‡Becton Dickinson Research Center, Research Triangle Park, NC 27709, U.S.A.

(*Received* 4 *November* 1994; *accepted* 16 *March* 1995)

Abstract—Modern automated drug-screening can generate hundreds of inhibitor leads from diverse chemical sources in a short period of time. Traditional methods of inhibitor analysis are resource intensive and limit the number of inhibitors that can be analyzed for their mechanism of inhibition. This paper presents methods we have developed for rapid estimation of both potency and mechanism of potential inhibitor leads for a biochemically complex screening target (protein kinase C) using commercially available computer programs for statistical experimental design. Our findings indicate that, with careful choice of factor levels, statistical experimental design clearly identifies the various interactions of the assay components with inhibitors. Suitably plotted, the data can be used to examine the competitive nature of the inhibitor and can provide estimates of IC_{50} and Michaelis constants useful for planning further kinetic work. The techniques used are amenable to automation and should be useful for identifying inhibitors that may have only marginal potency, but exhibit desirable mechanistic profiles suitable for structural analoging efforts.

Key words: kinetics; experimental design; screening; protein kinase C; enzymology; inhibition

Steady-state kinetic analyses have been used for decades to characterize mechanisms of enzyme inhibition. While traditional methodologies and mathematical treatments used for quantitative analysis, e.g. Michaelis–Menten kinetics, continue to serve enzymologists in the study of inhibitor mechanisms, the labor and resource intensive nature of these approaches limit their utility for evaluating a large number of inhibitors rapidly. Modern automated drug-screening assays have the potential to generate hundreds or even thousands of potential inhibitor leads in a short period of time. Most of these potential leads are usually eliminated through follow-up assays that determine IC_{50} values for a particular set of assay conditions. The most potent inhibitors are then characterized kinetically to determine their mechanism(s). In many cases, by the time the kinetic analyses are performed, considerable preparative or synthetic work on the screening lead by teams of chemists has been invested. While this approach may be satisfactory for simpler screens such as ligand binding to receptors, in more complex enzymatic assays this strategy runs the risk of overlooking promising candidates for development, which have desirable mechanistic profiles but lack potency, a property that can often be enhanced by examination of a compound's structure-to-activity relationship. Conversely, potent inhibitors are sometimes found to be reactive or destructive chemicals that interact with multiple assay components and are unsuitable for drug development. Therefore, one of the key issues facing enzymologists in high throughput enzyme-screening operations is an ability to rapidly and effectively characterize the mechanistic profiles of all the inhibitors generated by the screen.

The PKC§ (EC 2.7.1.37) family of lipid-regulated enzymes (reviewed in Refs. 1 and 2) is an excellent example of a complex biochemical screening target. This protein kinase family has been implicated in a variety of signal transduction pathways [2, 3], and the identification of isozyme selective inhibitors has been a focus of our screening efforts. In our laboratories, eight recombinant, baculovirus-expressed human PKC isozymes (α, β_1, β_2, γ, δ, ϵ, ζ, and η) have been screened in high throughput fashion against several thousand compounds. Kinetic analysis of these inhibitors has been limited to only the most potent inhibitors. However, even this limited subset has been difficult to analyze since the various isozymes have up to six cofactor or substrate variables that, in addition to their potential interactions with inhibitors, display interactions with each other [4]. The independent variables or factors in a PKC assay include phosphatidylserine, diacylglycerol, magnesium, ATP, protein substrate, and calcium for the Ca^{2+}-dependent members (α, β_1, β_2, and γ). To minimally describe inhibitor interactions with the various factors, traditional approaches to inhibitor analysis would require approximately 200 assay tubes/inhibitor (4 levels of factor in duplicate × 4 doses of inhibitor × 6 factors), and yet the results would not reveal information concerning interactions between, for example, any two of the factors and the inhibitor.

Recently, our group has been exploring the use of SED for rapid assay development and optimization [5, 6]. The SED approach to process development uses small, efficient experimental designs to collect informa-

† Corresponding author: Dr. Duane D. Bronson, Protein Chemistry, Sphinx Pharmaceuticals, Division of Eli Lilly, 4615 University Drive, Durham, NC 27717. Tel. (919) 489-0909; FAX (919) 489-1308.

§ Abbreviations: PKC, protein kinase C; SED, statistical experimental design; MBP, myelin basic protein; DG, 1,2-dioleoyl-sn-glycerol; PS, dioleolyl phosphatidylserine; SP4012, *trans*-3-(4-hydroxyamido)-4-[4-(2-hydroxy-6-hydroxycarbonylbenzoyl)-3,5-dihydroxybenzoyloxyl]pyrrolidinium trifluoroacetate; and PMSF, phenylmethylsulfonyl fluoride.

tion-rich data about factors that affect process performance. The experimental designs used in SED consist of matrices of *high* (coded as +1) and *low* (coded as −1) levels of independent variables (*factors*) arranged in factorial fashion (for two factors, +1+1, +1−1, −1+1, −1−1). To detect *curvature* or departure from linearity of a factor's effect and to add degrees of freedom for estimates of error, *midpoints* (coded as 0s) may be included for all factors. The experiment is performed according to the chosen design and the *response* (in our case, enzyme activity) is measured. The response is then analyzed by multiple regression on the coded factors, and estimates of *effects* [est. effect = avg(+ runs) − avg(− runs)] are generated. Deviations from simple addivity between any two effects can be interpreted as evidence of their *interaction* with each other [5].

The utility of the SED approach for enzymatic inhibitor analysis lies in its ability to detect the synergistic or antagonistic interactions between two assay components. There are many techniques used in enzyme kinetics which are based on the similar process of detecting parallel or intersecting plots (often linearized by inverse or log transformations) of [substrate] versus velocity data at varying levels of antagonists or agonists. Interpretation of these various plots is the general way in which an inhibitor or activator is assigned its so-called "mechanism" of action. By inspecting interaction plots and the response surface plots generated by estimated second degree polynomials used to fit the regression models, qualitative information equivalent to that obtained by traditional kinetics can be generated using SED methods.

Where there are many factors affecting a process, statisticians have developed fractional factorial and other designs to minimize the number of samples or *runs* necessary to estimate the effects of factors on a given process and defined the *confounding patterns* (inability to independently estimate effects) that result from decreased numbers of runs. Extensive literature about SED, the statistical analyses used, their validity or accuracy, and its limitations are available [5, 6].

During our evaluation of SED for assay development, we used our PKC assay as a test case. The data we gathered agreed very well with observations we had made previously using conventional approaches. This result led us to ask the following question: If an enzyme inhibitor was included in the experimental design as an assay factor, would the results generated by an SED approach elucidate the mechanism(s) of inhibition? The following study was designed to address this question. For the model inhibitor, we chose a potent synthetic analog of balanol [7], a natural product discovered in our high throughput enzymatic screen.

MATERIALS AND METHODS

Reagents

PS and DG were obtained from Avanti Polar Lipids; [γ-^{32}P]ATP was from DuPont-New England Nuclear; staurosporine was from Boehringer Mannheim; and bovine brains were obtained from Pel-Freez Biologicals. All other chemicals were of reagent grade. All purification procedures were done at 0–4°.

Myelin basic protein

MBP was prepared by modifications of existing methods [8, 9]. Bovine brains were weighed and homogenized in 10 vol. (w/v) buffer (10 mM Tris, pH 8, 0.85 M sucrose, 1 mM EDTA, 0.1 mM PMSF) using a blender. The homogenate was centrifuged at 17,000 *g* for 1.5 hr to float the myelin. Aspirated myelin was diluted 10-fold (v/v) in buffer without sucrose and supplemented with 2% TX-100 to extract phospholipids. After 15 min, the suspension was centrifuged at 17,000 *g* for 1 hr. The pellets were washed three times in 5 vol. buffer without detergent, using a Polytron homogenizer to resuspend, and centrifuged at 17,000 *g* for 30 min. The washed pellets were resuspended in 10× (v/v) extraction buffer (50 mM sodium acetate, 500 mM NaCl, 0.1 mM EGTA, 0.1 mM PMSF, pH 4.5) and stirred overnight. The extract was clarified by centrifugation at 17,000 *g* for 1 hr and applied to a Perseptive Biosystems POROS 50HS strong cation exchange column equilibrated with 20 mM sodium phosphate buffer, pH 7.5. The column was washed with 10 column volumes of buffer and step eluted with buffer containing 1 M NaCl. Purity by SDS–PAGE was >90%.

Protein kinase C-δ

Spodoptera frugiperda (SF9) insect cells were infected with recombinant Baculovirus containing PKC-δ [10] and grown in large scale [11] as previously described. For partial purification, a 10-mL cell pellet (~2 × 10^7 cells) was thawed and diluted to 100 mL with homogenization buffer (50 mM Tris, pH 8.0, 250 mM sucrose, 2 mM EDTA, 1 mM EGTA, 1 mM dithiothreitol, 1 mM PMSF, 20 μg/mL leupeptin). Cells were homogenized using a Wheaton medium-fit motorized teflon/glass dounce at 1730 rpm for 5 strokes. The homogenate was centrifuged at 33,000 *g* for 20 min. The supernatant was adjusted to 50% saturation with ammonium sulfate and pelleted at 33,000 *g* for 30 min. The pellet was resuspended in 100 mL column buffer (25 mM Tris, pH 8.0, 1 mM $MgCl_2$, 1 mM dithiothreitol, 0.1 mM EGTA, 1 μM $ZnCl_2$, 10% glycerol) using a Wheaton tight-fit (A) glass dounce and centrifuged at 33,000 *g* for 15 min to clarify. The supernatant was applied to a 25-mL POROS 50HQ strong anion exchange column equilibrated with chromatography buffer at 10 mL/min. The column was washed with 5 column volumes of buffer, and protein was eluted with a 250-mL gradient from 0 to 1.0 M NaCl. Enzyme fractions were screened for PKC activity ± lipids and pooled accordingly. The concentration of protein in the pool was determined by the BioRad method to be 1.48 mg/mL using γ-globulin as a standard. Purity was estimated by SDS–PAGE to be ~20%. The decision to use an impure preparation was governed by our desire to develop a testing model reflective of our screening assay. The preparation used was free of endogenous substrates (no measurable activity above background in the absence of MBP), other kinases (SF9 cells are known for their low level of endogenous PKC [10] and all activity was DG-dependent), ATPases (monitored by thin-layer chromatography), proteases (preincubation of enzyme for 30 min at 37° showed no loss in activity), and phosphatases (30 min post-incubation of balanol stopped assay showed a negligible decrease in precipitable counts). The presence of inactive carrier enzyme was not ruled out.

General assay methods

To prepare small phospholipid vesicles, appropriate amounts of PS and DG stocks in chloroform were added

to a glass tube and dried under N_2. Assay buffer (35 mM HEPES, pH 7.0, 0.08 mM EGTA) was added, and the solution was probe-sonicated 2 × 30 sec at 30% of maximal power using a Heat Systems Sonic Dismembrator with vortexing between sonications. For the screening design, five vesicle preparations differing in their PS:DG ratios were used. To perform the assay, components were added in the following order: vesicles in buffer, H_2O, compound in DMSO, MBP, [γ-^{32}P]ATP stock (300 μM; 0.05 Ci/mmol; supplemented with 100 mM $MgCl_2$) and 0.75 μg crude enzyme to start the assay. Total assay volume was 0.25 mL. For assays that required higher ATP levels, unlabeled ATP from a buffered stock solution was added in place of some of the water. The reaction was incubated at 30° for 10 min and stopped by the addition of 0.5 ml of 25% ice-cold trichloroacetic acid (TCA); 100 μL of 1 mg/mL BSA was added as a carrier, and the mixture was filtered on GFC-type filter mats using a TomTec Cell Harvester specially modified to handle concentrated TCA. The filter was dried and bagged with 10 mL of scintillation fluid (Betaplate Scint, Wallac). ^{32}P was detected by a Wallac 1205 Betaplate liquid scintillation counter.

Statistical analyses

All experimental designs, statistical analyses and graphical representations of data were generated using Manugistic's STATGRAPHICS PLUS© (Statistical Graphics Inc., v.7.0, DOS) and StatSci's S+DOX© (MathSoft Inc., v.1). For screening designs and their associated calculations, these programs use methods described in Refs. 5 and 6. Response surface methodologies used are based mainly on those described in Ref. 12. Several manufacturers are currently offering statistical packages containing SED software. These programs greatly simplify the application of the processes used in the SED approach.

Experimental designs

Since the balanol analog SP4012 inhibits both Ca^{2+}-dependent and Ca^{2+}-independent isozymes of PKC, we decided to use the Ca^{2+}-independent PKC-δ as our model enzyme. This limited the number of factors under study and reduced the size of the design. Mg^{2+} was held at 10 mM for similar reasons and because, in addition to its catalytic role as an ATP binding cofactor, this cation plays a physical role in our PKC assay by helping to aggregate vesicles, protein substrate, and ATP [13].

A wide variety of factorial and fractional factorial designs has been developed by statisticians. The fractional designs balance *resolution* (ability to clearly assign and estimate effects) with number of runs (the limiting factor when measuring complex processes) and contribute flexibility to the SED approach. The SED design chosen to analyze the four cofactor/substrates ± inhibitor was a fractional factorial using 16 of the 2^5 possible runs from the full factorial. This design is shown in non-randomized coded form in Table 1 along with its factor settings and response values. The design was run with three centerpoints and randomized to prevent systematized error, but all inhibitors in a given experiment used the same layout to allow for multi-channel pipetting. The design was of Resolution V, meaning that all main effects and two-factor interactions can be estimated without confounding [6].

The choice of factor levels is crucial to success in SED [5]. For PKC we chose values that reflect both PKC literature values (e.g. [4]) and data generated in our screening efforts (not shown). For the regulatory lipids, PS and DG, 5- and 10-fold ranges, respectively, around empirically determined inflection points (where activity is nearly saturated) were used. These points are determined in an iterative fashion as part of quality assurance protocols to assure steady-state kinetics and are specific for this preparation of PKC-δ in our screening assay. The ranges used ensured that the low value was below half-V_{max}, the midpoint was well above that point (near V_{max}), and the high value was at V_{max} for these regulatory factors.

Kinetic interactions between substrates are common in multisubstrate systems [14]. The concentrations chosen for the two substrates, ATP and MBP, were based on the following: (1) Because of cost and radioactivity safety concerns, our screening assay uses 0.5 μCi ^{32}P/tube for PKC and achieves a target activity by titrating enzyme and protein substrate to ensure steady-state behavior (≤5% phosphotransfer within 10 min). This provides a sufficient counting window (~50,000 cpm) for reliable measurement of the response and economizes reagent usage. Kinetic data from other experiments (not shown) indicated that a 10-fold increase in carrier ATP (from 30 to 300 μM) usually results in a 2- to 3-fold decrease in the cpms observed with another 3- to 4-fold decrease occurring when ATP was increased another 10-fold. To prevent collapse of our counting window by inhibitors, we decided to use 300 μM ATP as our high value. This amount is sufficient for near V_{max} behavior at the lower setting of MBP; (2) MBP was varied 10-fold centered about a previously determined K_m ~30 μM at 300 μM ATP. For 30 μM ATP, the middle and upper values are saturating levels of substrate. Together, these settings explore most of the interactions between the two substrates and correlate the model for inhibitor interactions to our screening assay where inhibitors are first detected.

Although the above cofactor/substrate concentrations allowed a larger range of inhibitor concentrations to be tested, they also introduced curvature into the response surface owing to enzymatic saturation. Because the regression model used in SED assumes linearity of response with respect to individual factor effects, it was necessary to perform an inverse transformation on the response values for clear interpretation of the results. A similar inversion strategy is used in the double-reciprocal analysis [15] commonly used in Michaelis–Menten kinetics.

Since SP4012 (Fig. 1) is a racemic synthetic balanol analog generated in-house (Patent Application: WO9303730-A1; Derwent 93-093702/11, Sphinx Pharmaceuticals), IC_{50} values for each isozyme (~5 nM for delta) were generated in our standard assay. In addition, our group had generated kinetic data from other balanols (not shown), which indicated that they were ATP-competitive and displayed variously uncompetitive and non-competitive inhibition with regard to protein substrates. These preliminary assays were used to choose the 100-fold range of SP4012 used in the statistical designs.

RESULTS

The responses from the fractional factorial screening design are shown in Table 1 as reaction velocity in pi-

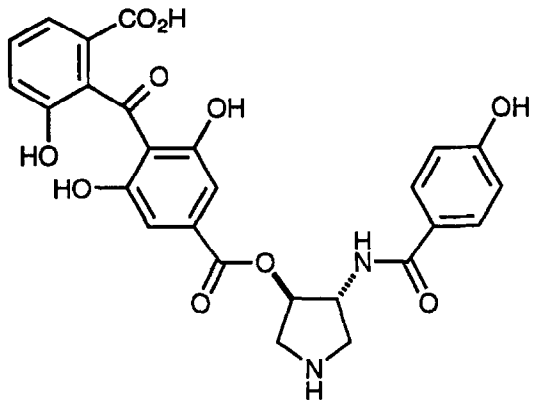

Fig. 1. Structural formula for SP4012, a balanol analog [*trans*-3-(4-hydroxyamido)-4-[4-(2-hydroxy-6-hydroxycarbonylbenzoyl)-3,5-dihydroxybenzoyloxyl]pyrrolidinium trifuloroacetate].

comoles per minute. In SED, a multiple regression approach is used to estimate the significance of a factor's effect on a process. For comparative purposes, the estimated effects are commonly plotted as a bar chart of their absolute values. This plot is known as a Pareto plot [5]. In this type of design, all of the available degrees of freedom (= number of runs) are used to estimate effects. Hence, there is no classical estimate of the experimental error available. However, the Pseudo Standard Error [16, 17] provides an alternative measure of the error. Critical values for comparing effects against the error are available in S + DOX and were used to draw the vertical line on the Pareto plot for $\alpha = 0.05$. Values to the right of this line are considered to have a <5% chance of rejecting a null hypothesis (the factor has no effect) when it is true.

Pareto plots for the inverted responses and factors (except the inhibitor) for control and experimental treatments are shown in Fig. 2. In the control experiment, the important effects that change PKC-δ activity are MBP and ATP. Their interaction is the next largest factor, but

Table 1. Fractional factorial design*

Experimental design						Reaction velocity (pmol/min)	
Run	A	B	C	D	E	Control	SP4012
1	−1	−1	−1	−1	+1	9.19	0.80
2	−1	−1	−1	+1	−1	17.08	27.87
3	−1	−1	+1	−1	−1	36.13	29.47
4	−1	−1	+1	+1	+1	68.32	8.61
5	−1	+1	−1	−1	−1	14.82	15.58
6	−1	+1	−1	+1	+1	21.99	13.82
7	−1	+1	+1	−1	+1	54.43	1.94
8	−1	+1	+1	+1	−1	85.65	79.45
9	+1	−1	−1	−1	−1	9.48	7.81
10	+1	−1	−1	+1	+1	11.91	7.47
11	+1	−1	+1	−1	+1	35.86	1.15
12	+1	−1	+1	+1	−1	52.01	39.41
13	+1	+1	−1	−1	+1	8.14	0.58
14	+1	+1	−1	+1	−1	18.50	15.99
15	+1	+1	+1	−1	−1	42.57	40.25
16	+1	+1	+1	+1	+1	87.62	12.24
17	0	0	0	0	0	58.71	9.58
18	0	0	0	0	0	68.17	9.10
19	0	0	0	0	0	74.29	8.78

Factor levels:	low (−1)	mid (0)	high (+1)
A: PS (μM)	30	90	150
B: DG (nM)	16.7	91.8	167
C: MBP (μM)	5.5	30.5	55.5
D: ATP (μM)	30	165	300
E: Inhibitor (nM)	1	50.5	100

* Shown is the experimental design of the fractional factorial type for 5 factors used for analysis of inhibitor interaction with PKC. Factor levels are set according to the schedule shown.

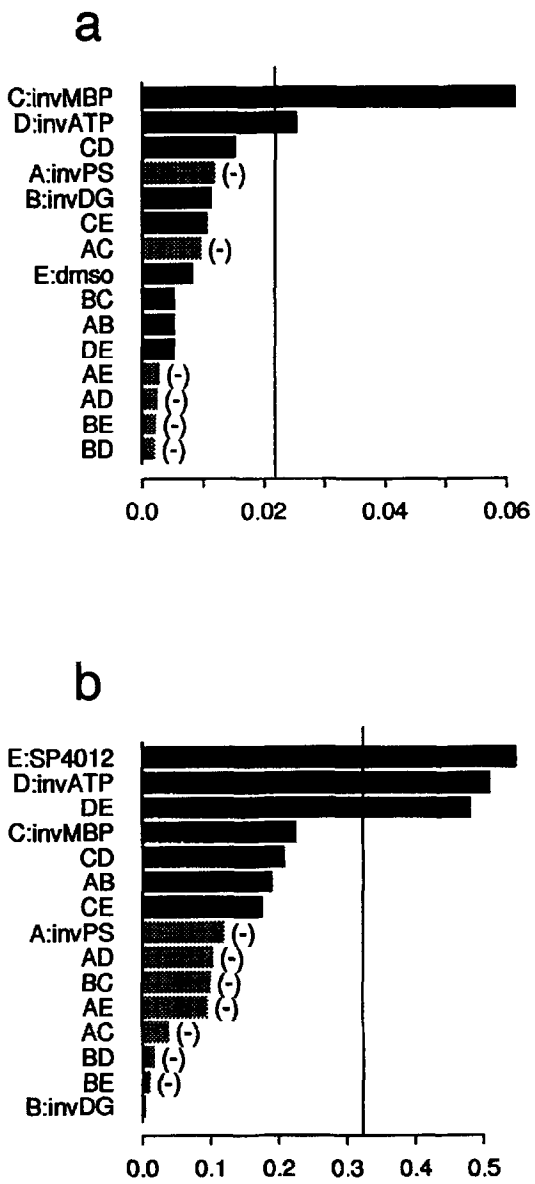

Fig. 2. Pareto plots of the inverted data from the five-factor fractional factorial design for control (a) and inhibitor (b) treatments on PKD-δ activity. This plot was generated using S + DOX and shows the absolute value of the estimated effects in rank order. The letters for specific two-way interactions follow the example: CD = [interaction between invMBP (C) and invATP (D)]. The dotted fills are for negative effects, the solid for positive ones. The vertical line represents $\alpha = 0.05$. Values to the right of this line are considered highly significant. Units are min/pmol.

it is not quite significant at $\alpha = 0.05$. Inspection of the inverted response with the inhibitor SP4012 present demonstrated the inhibitor and ATP to be substantially more important than MBP and indicated that a statistical interaction of ATP with the inhibitor seems highly significant. It should be noted that the inversion of the factors in a model such as this results in a sign change in the estimated effects since factor levels (except inhibitor) are now going from high to low.

Interaction plots [5] are a means of examining estimated responses at high and low settings of other factors as one factor increases on the x-axis. Converging or crossing lines for the two settings indicates an interaction between factor pairs. Inspection of these plots for the inverted data with SP4012 (Fig. 3a) and ATP (3b) demonstrated that SP4012 behaves like the "inverse" of ATP that is, 3(a) and 3(b) show the same pattern of interactions. Plots of MBP (3c) and PS (3d) show that SP4012 and inverse-ATP had similar interactions with these factors as well (CD, CE in Fig. 3a and AD, AE in Fig. 3b). Significant interactions between DG and either ATP or SP4012 were absent and plots of the sham inhibitor treatment showed no significant interactions of the DMSO with any other factors (not shown).

Preliminary investigations into other balanols indicated a competitive mechanism for ATP and both non-competitive and uncompetitive kinetics regarding MBP and other protein substrates using narrow and broad ranges of inhibitor concentrations, respectively (not shown). Recent work in another laboratory on balanol isolated from a different organism [18] also indicated an ATP-competitive mechanism that was uncompetitive for protein substrate. To better resolve the issue of how this inhibitor interacts with the two substrates and which factors had the largest contributions to the curvature observed as V_{max} was approached, a response surface design of the Box–Behnken type [12] was employed. A control inhibitor, staurosporine, previously shown to be ATP-competitive [19], was included in this experiment. The results for this experiment are shown in Table 2, and Pareto plots for the effects calculated from the inverted responses are shown in Fig. 4(a–c). Significant effects are those that fall to the right of the vertical line, which for this design is based on the standard t-test. In this response surface design, an inversion of the factor levels is not possible because their centerpoints are severely displaced by the inversion. The main effects and interactions that characterized the screening design were evident in this experiment (although the mathematical signs are changed). Additionally, a strong curvature term for ATP was seen when the inhibitors were present (term BB in Fig. 4,b and c). Note that the plots for SP4012 and for staurosporine are almost superimposable.

Response surface plotting [12] offers an intuitive picture of the estimated effects between two factors because it shows all of the estimates between end-points as a curved or planar surface. These surfaces can be generated using various combinations of values for the other factors. Figure 5a shows a plot of the estimated response from the DMSO control fractional factorial inverted data against both MBP and ATP. The PS, DG and DMSO factors are set to the midpoints. Side views of this plot suggest that both V_{max} and K_m are changed in a fashion reminiscent of double-displacement kinetics [14]. Figure 5b shows a response surface plot estimated using the

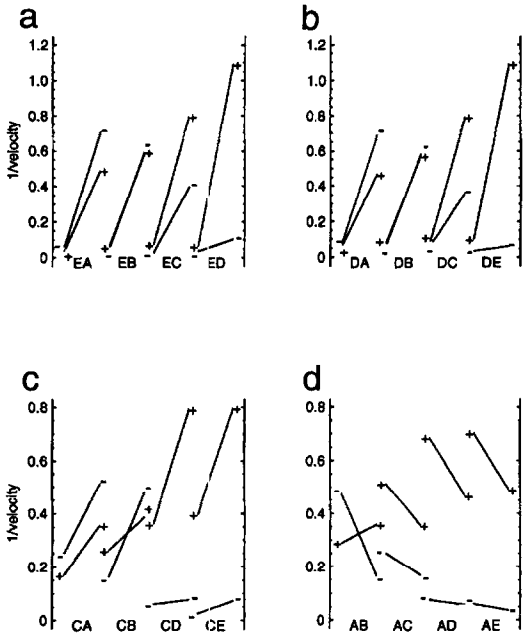

Fig. 3. Interaction plots of the inhibitor E:SP4012 (a), D:ATP (b), C:MBP (c) and A:PS (d) with each of four other factors from the fractional factorial design. In this type of plot, the common factor is plotted on the x-axis going from low to high settings, and the estimated response is plotted for the low (–) and high (+) settings of the other factors on the y-axis. If the plot results in parallel lines, there is no interaction between the factors. Crossing or converging plots are indicative of interactions. In this figure, the inverted data are used for the response and all factors except E:SP4012. Factor B is DG. Units are in min/pmol.

Table 2. Response surface design*

Experimental design				Reaction velocity (pmol/min)		
Run	A	B	C	DMSO	SP4012	Staurosporine
1	–1	–1	0	24.33	12.84	19.27
2	+1	–1	0	24.35	0.50	0.85
3	–1	+1	0	48.87	25.31	31.64
4	+1	+1	0	39.70	3.62	5.21
5	–1	0	–1	15.81	10.20	13.88
6	+1	0	–1	14.27	1.64	3.10
7	–1	0	+1	61.05	46.62	54.48
8	+1	0	+1	53.04	2.65	4.31
9	0	–1	–1	10.39	0.44	0.82
10	0	+1	–1	23.54	5.37	7.74
11	0	–1	+1	33.52	0.95	1.70
12	0	+1	+1	62.02	7.77	11.52
13	0	0	0	29.60	2.73	5.76
14	0	0	0	45.40	4.52	6.79
15	0	0	0	43.75	3.61	6.13

Factor levels:	low (–1)	mid (0)	high (+1)
A: Inhibitor (nM)	1	50.5	100
B: ATP (μM)	30	165	300
C: MBP (μM)	5.5	30.5	55.5

* Shown is the experimental design for response surface analysis of inhibitor mechanism using a 3 factor Box-Behnken layout. As in Table 1, factor levels are set according to the schedule shown.

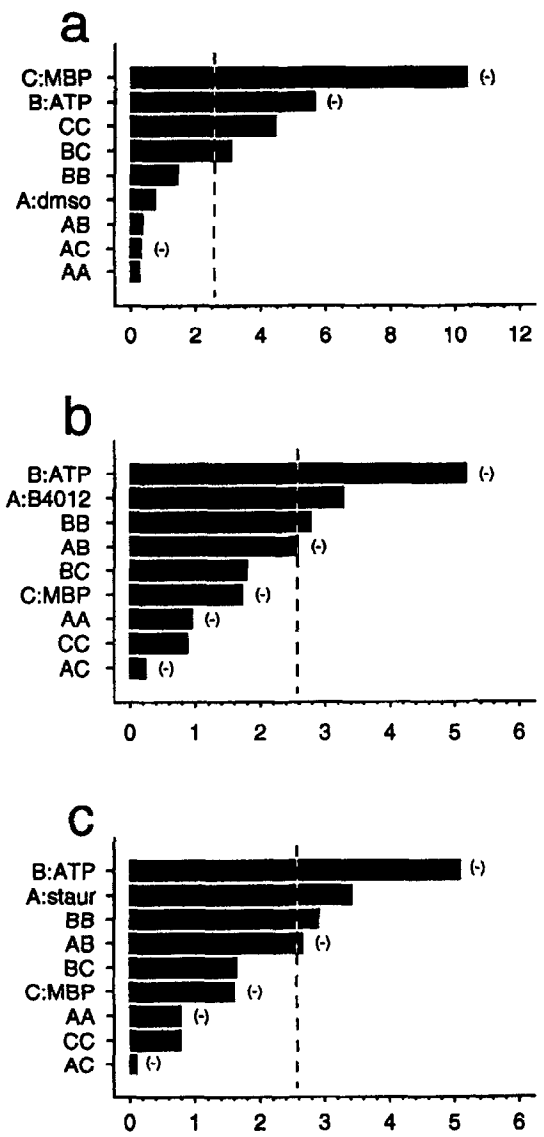

Fig. 4. Pareto plots of the inverted responses from the Box–Behnken design for inhibitor analyses of PKC-δ. These plots were generated with STATGRAPHICS PLUS using the standardized Pareto chart option. The plot is of the absolute effects divided by the total error and the line is generated for $\alpha = 0.05$. Key: (a) control, (b) SP4012 and (c) staurosporine. In addition to the two-way interaction code as in Fig. 2, this figure includes quadratic terms for curvature estimation [e.g. BB = curvature term for ATP (B)]. Units are multiples of the total experimental error.

inverted data from the fractional factorial design for the interaction between ATP and SP4012 using midpoint values for other factors. Inhibitor interactions with other components (not shown) yield planar (PS and DG) or only slightly curved surfaces (MBP). In the case of MBP, the interaction with SP4012 decreased as the concentration of ATP used in estimating the response was raised.

Response surfaces can also be generated at multiple settings of one factor and subsequently combined into a single plot. This was done for 0.0 and 50.5 nM levels of SP4012 versus ATP and MBP using the inverted fractional factorial data (Fig. 5c). This graph suggests a competitive mechanism of inhibition with respect to ATP at both high and low levels of MBP but shows noncompetitive inhibition and uncompetitive inhibition with MBP at low and high levels of ATP, respectively. An aggregate plot of the inverted response surface design at 1, 50.5, and 100 nM concentrations of SP4012 is shown in Fig. 5d. The tendency of the surfaces to "peel" away at low concentrations of ATP suggests that this factor is much more important for overcoming inhibition than is the MBP.

DISCUSSION

The activity of an enzyme in any assay is dependent on the effects of assay factors and their interactions, and the total experimental error. SED was developed by statisticians as a set of mathematical tools capable of addressing the signal to noise issue for a variety of processes. Its utility for optimization of biological assays is well documented [5]. While using SED to optimize our PKC assay and because of the similarity between the observed statistical interaction plots of PKC's substrates/co-factors and traditional kinetic plots of these same factors that were generated previously, we realized that these approaches could be adapted to inhibitor studies.

PKC shows double-displacement kinetics with respect to its two substrates, ATP and protein/peptide [4]. In double-displacement kinetics, when one substrate is varied at different levels of the other, the K_m and V_{max} for the other substrate change proportionately, resulting in parallel double-reciprocal plots of the data. This behavior is generally interpreted as being due to either an acyl intermediate, induced fit (e.g. hexokinase), or an ordered mechanism [14]. Which mechanism(s) governs PKC activity is unclear, but studies utilizing the isolated catalytic subunit apparently showed an ordered sequential mechanism suggesting that the double-displacement behavior might be due to regulatory subunit interactions [4]. Regardless of its mechanistic origin, the double-displacement behavior complicates the analysis of inhibitors that interact with either of the substrate binding sites.

In our laboratory we have analyzed a number of compounds that interact with the nucleotide binding site of PKC. Presumably because of varying protein substrate specificities seen among the various PKC isozymes and their double-displacement kinetic behavior (which we have observed for all isozymes), we have often found the interpretation of inhibitor interactions with protein factors tedious and confusing. The ability of the SED approach to detect both noncompetitive and uncompetitive behavior within a single experiment (Fig. 5c) emphasizes the need for caution in interpreting the results of studies in multisubstrate systems. This is because the protein conformational interplay (interaction) between substrate/cofactor binding sites complicates (confounds) the mechanistic interpretation of inhibition. In the present study, analyses of the interaction patterns of the inhibitor SP4012 (Figs. 3 and 5b) suggest that this compound is a simple competitive inhibitor with respect to ATP and that other competitive profiles are simply reflections of the interactions of ATP with other components and the enzyme (PKC) in the assay. The ability of SED inhibitor analysis to clearly separate these interactions from each other represents a distinct advantage of this approach.

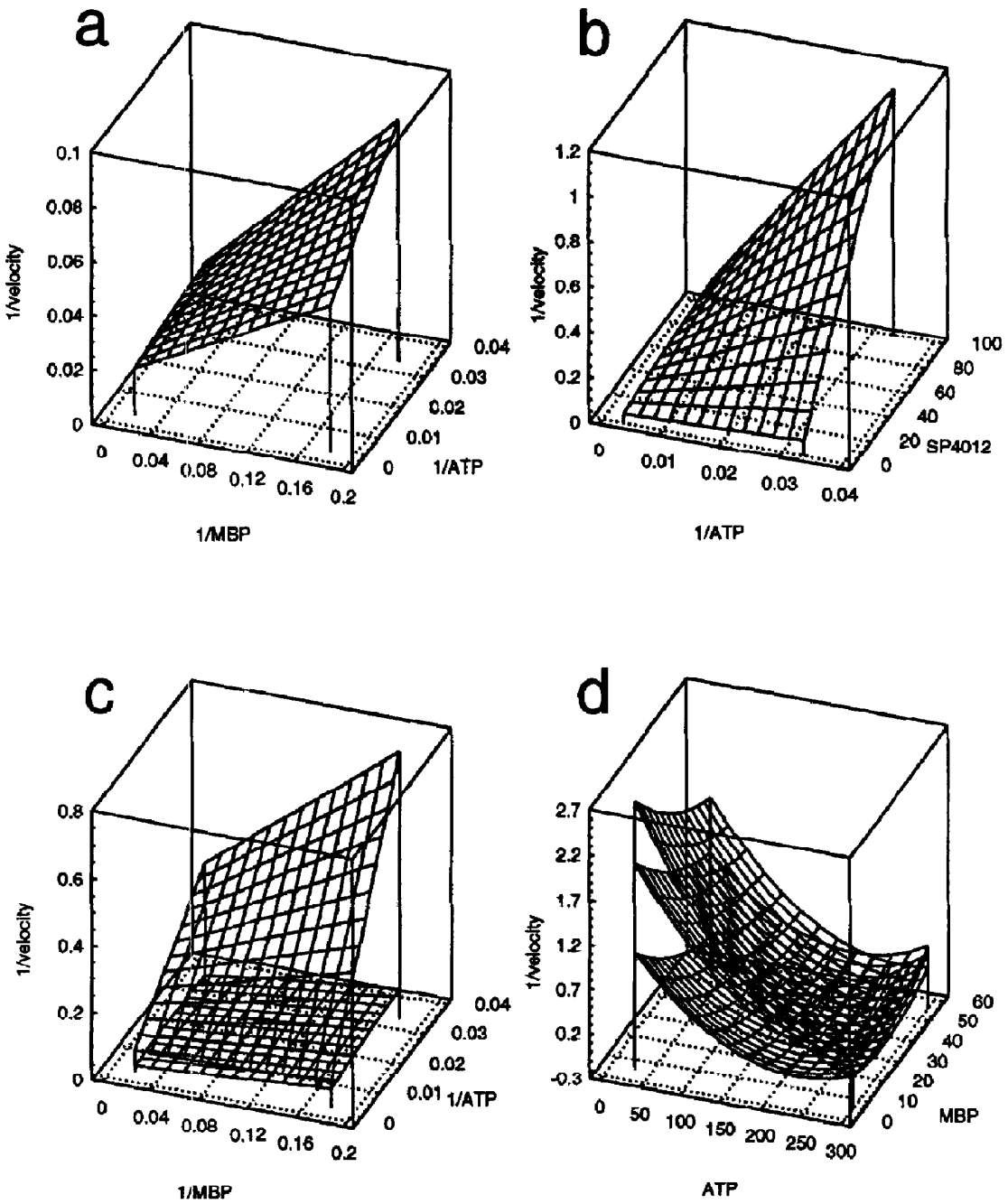

Fig. 5. Response surface plots generated using STATGRAPHICS PLUS. All plots were generated with non-varied factors set at their midpoints. (a) Double-reciprocal type plot for control PKC-δ activity as MBP and ATP are varied. Side views are suggestive of double-displacement kinetics. (b) Plot of activity as SP4012 and ATP are varied against each other. If viewed from the front face (1/ATP), this plot suggests that SP4012 is a competitive inhibitor with respect to ATP. (c) Composite plot similar to that in (a) but additionally showing the SP4012 at 50.5 nM. For the MBP, note the convergent pattern of noncompetitive inhibition at low ATP levels, which converts to the parallel lines of uncompetitive inhibition as ATP levels rise. (d) Composite response surface plot of 1, 50.5 and 100 nM concentrations of SP4012. The increased sensitivity of the assay to inhibition at low ATP levels is apparent.

We selected PKC as a model system to apply these techniques to both for its complexity and because we possessed a large amount of information about PKC activity from published literature and in-house efforts. The factor levels chosen in this study reflect this information and are responsible for the good "fit" of the data to the chosen models.

It is realized that this level of information will not be readily available for most activities. The inhibitor assay should vary the chosen factors about a "center" value determined by the screening assay levels. Decisions have to be made about which factors in the assay to vary, since estimated statistical interactions are obtainable only for varied factors. For most screens, it will be the

substrates and cofactors that are of interest mechanistically. Our strategy of varying these levels about inflection points near V_{max} on the activity curve seems to have worked well for PKC. The idea was to make the assay both more and less sensitive to inhibitor effects and extend the range over which a standard dilution of inhibitor could provide useful information.

The critical unknown factor when using SED as a tool for high throughput inhibitor analysis will be the potency of the inhibitor. By running a solvent control design with each assay, SED inhibitor analysis collects direct information about four levels of compound (none, low, mid, and high) at two or three levels of each substrate/cofactor. In the PKC example, we have used 20× the IC_{50} of SP4012 as our high level and 0.2× as our low. These levels mimic a "hit" that dilutes out within two orders of magnitude to a level below its IC_{50}. Because greater dilutions tend towards the control set of uninhibited values, little qualitative mechanistic information is lost. The estimable response space is simply restricted and statistical confidence decreases. When SP4012 was run in a Box–Behnken design at 1, 5 and 10 nM (−1, 0, +1) levels, the same trends were found as in the larger range (not shown). However, if the dilution is insufficient to substantially remove the inhibition, then it is not possible to estimate main effects or interactions. When this occurs, there is no choice but to lower the settings of the inhibitor and run another experiment. This can be avoided by running the design with multiple dilutions of each inhibitor and choosing the proper set to analyze or by first performing an IC_{50} determination at the running concentrations of substrates and cofactors for the primary assay (the center of the inhibitor design) prior to the mechanistic screen.

Although we have used the inverse velocity and/or factors to linearize our data for fitting the regression model, other options, such as log plots, could be used. Response surface designs can be linearized by these transformations as well if care is taken to offset the centerpoints in an appropriate fashion. Regular activity plots can also provide useful information if response surface designs (which are sensitive to curvature) are used or only linear portions of the response are looked at.

A wide variety of analyses and plotting options are available with various SED software packages. In addition to an array of useful plots, relevant kinetic constants can usually be directly estimated (including the IC_{50}, K_m and V_{max}) from the regressions and used to guide an inhibitor's analysis. Programmable statistical packages also allow other constants (such as K_i) to be estimated. The ease of directly and automatically obtaining these estimates, with their appropriate confidence intervals, varies from one software package to another. Careful consideration should therefore be paid to these issues when choosing an analysis package. It should be emphasized that the techniques in this approach are not a substitute for thorough kinetic analyses of a screen's most promising leads but are, instead, methods for focusing one's limited analytical resources towards those leads.

We have looked at other inhibitors of PKC using the paradigms outlined in this study (not shown). Sphingosine is an inhibitor of PKC [20], thought to interact with the lipid regulatory domain of the enzyme. Analyses similar to those presented here showed competitive interactions between this inhibitor and both lipids, PS and DG. Interestingly, the screening design also detected a competitive interaction of this compound with MBP, probably caused by direct binding of the compound to hydrophobic sites on this membrane binding protein, since the catalytic and regulatory sites are located on separate protein domains in PKC. Some other inhibitors we examined were polylysine and polyarginine, compounds known to be competitive inhibitors with respect to PKC protein substrate [21]. In these cases, the most important interactions were found to be those between the protein substrate and the inhibitors, although interactions between the polyamines and the charged components, ATP and PS, were also present.

In summary, our preliminary experiences with SED inhibitor analyses indicate that these approaches may have great utility for the rapid classification of inhibitor mechanisms for leads generated in high throughput enzymatic screens. Both the designs themselves and the statistical analyses used are amenable to automated procedures. SED approaches may also be useful for analysis of agonists.

Although it is clear that more work with a variety of other screening target/inhibitor combinations needs to be done so that statistical profiles of all types of enzyme inhibition can be recognized, the promise of the SED approach is apparent. Using these methods, an enzymatic screen could be run at a fairly high "hit" rate and followed by an assay designed to winnow these compounds further according to their mechanistic profiles. The result would be a reduction in the resources necessary to identify quality leads for potential drug development.

Acknowledgements—The authors wish to thank Carson Loomis and Bill Janzen for helpful discussions on PKC and inhibitor interactions and the Screening Group at Sphinx for generating so much information on PKC. We would also like to thank Robert Crowl for his question: "So if you plugged an inhibitor in as a factor, this thing could tell you the mechanism of inhibition . . . right?"

REFERENCES

1. Parker PJ, Kour G, Marais RM, Mitchell F, Pears C, Schaap D, Stabel S and Webster C, Protein kinase C–A family affair. *Mol Cell Endocr* **65:** 1–11, 1989.
2. Nishizuka Y, The family of protein kinase C for signal transduction. *JAMA* **262:** 1826–1832, 1989.
3. Nishizuka Y, Intracellular signalling by hydrolysis of phospholipids and activation of protein kinase C. *Science* **258:** 607–614, 1992.
4. Hannun YA and Bell RM, Rat brain protein kinase C: Kinetic analysis of substrate dependence, allosteric regulation and autophosphorylation. *J Biol Chem* **265:** 2962–2972, 1990.
5. Haaland PD, *Experimental Design in Biotechnology.* Marcel Dekker, New York, 1989.
6. Box GEP, Hunter WG and Hunter JS, *Statistics for Experimenters.* Wiley, New York, 1978.
7. Kulanthaivel P, Hallock YF, Boros C, Hamilton SM, Janzen WP, Ballas LM, Loomis CR, Jiang JB, Katz B, Steiner JR and Clardy J, Balanol: A novel and potent inhibitor of protein kinase C from the fungus *Verticillium balanoides. J Am Chem Soc* **115:** 6452–6453, 1993.
8. Bellini T, Rippa M, Matteuzzi M and Dallocchio F, A rapid method for purification of myelin basic protein. *J Neurochem* **46:** 1644–1646, 1986.
9. Riccio P, Liuzzi GM and Quagliariello E, Lipid-bound, native-like myelin basic protein: Batch-wise preparation

and perspectives for use in demyelinating diseases. *Mol Chem Neuropathol* **13:** 185–193, 1990.

10. Rankl N, Rice J, Gurganus T, Barbee J and Burns D, The production of an active protein kinase C-delta in insect cells is greatly enhanced by use of the basic protein promoter. *Prot Expr Purif* **5:** 346–356, 1994.
11. Rice JW, Rankl NB, Gurganus TM, Marr CM, Barna JB, Walters MM and Burns DJ, A comparison of large-scale Sf9 insect cell growth and protein production: Stirred vessel vs. airlift. *Biotechniques* **15:** 1052–1059, 1993.
12. Box GEP and Draper NR, *Empirical Model Building and Response Surfaces.* Wiley, New York, 1987.
13. Bazzi MD and Neltsestuen GL, Autophosphorylation of protein kinase C may require a high order of protein–phospholipid aggregates. *J Biol Chem* **267:** 22891–22896, 1992.
14. Fersht A, *Enzyme Structure and Mechanism.* Freeman, New York, 1985.
15. Lineweaver H and Burk D, The determination of enzyme dissociation constants. *J Am Chem Soc* **56:** 658–666, 1934.
16. Lenth RV, Quick and easy analysis of unreplicated factorials. *Technometrics* **31:** 469–473, 1989.
17. Haaland PD and O'Connell MA, Inference for effect-saturated fractional factorials. *Technometrics* **37:** 82–93, 1995.
18. Ohshima S, Yanagisawa M, Katoh A, Fujii T, Sano T, Matsukuma S, Furumai T, Fujiu M, Watanabe K, Yokose K, Arisawa M and Okuda T, *Fusarium merismoides* Corda NR 6356, the source of the protein kinase C inhibitor, azepinostatin: Taxonomy, yield improvement, fermentation and biological activity. *J Antibiot (Tokyo)* **47:** 639–647, 1994.
19. Tamaoki T, Nomoto H, Takahashi I, Kato Y, Morimoto M and Tomita F, Staurosporine, a protein inhibitor of phospholipid/Ca^{++} dependent protein kinase. *Biochem Biophys Res Commun* **135:** 397–402, 1986.
20. Hannun YA, Loomis CR, Merrill AH and Bell RM, Sphingosine inhibition of protein kinase C activity and of phorbol dibutyrate binding *in vitro* and in human platelets. *J Biol Chem* **261:** 12604–12609, 1986.
21. Leventhal PS and Bertics PJ, Kinetic analysis of protein kinase C: Product and dead-end inhibition studies using ADP, poly(L-lysine), nonhydrolyzable ATP analogues, and diadenosine oligophosphates. *Biochemistry* **30:** 1385–1390, 1991.